

Turbulent Base Heating on a Slender Re-Entry Vehicle

W. LEON FRANCIS*

Aeronutronic Division, Philco-Ford Corporation,
Newport Beach, Calif.

THE purpose of this Note is to report on some turbulent base heating measurements obtained from flight tests of a very slender re-entry vehicle. This unique data is limited in scope since the measurements were obtained primarily as diagnostic information. Data accuracy is estimated to be $\pm 10\%$. A single copper slug calorimeter was used to obtain base heating rates on each of seven flights of nearly identical vehicle configurations, but on two different re-entry trajectories. Vehicle characteristics include a half-cone angle of 4.5° , nose bluntness ratio $= 0.035$ (graphite nose tip), and either a phenolic silica or phenolic carbon heatshield on the seven foot long flat-based vehicles. Re-entry performance was generally nominal for the two typical ballistic re-entry trajectories given in Table 1.

The calorimeter copper slug used a copper-constantan thermocouple bead soldered to the backface of the slug on all flights except the first. No correction was made for temperature gradients in the slug. The reliable calibration limit is 555°F . Data above this limit are not included. On the first flight, a resistance thermometer gage was bonded to the slug backface. This vehicle was the only one with the base heating measurement at a relative base radial station, $R/R_b = 0.66$. All other flight measurements were made at $R/R_b = 0.22$. Due to the lower heating rates on flight one, data were obtained to impact. Data reduction was performed only for altitudes of 100,000 ft and below, relating primarily to the turbulent flow regime. Smoothing of raw temperature data was performed manually, and the resultant temperatures fit to a second order polynomial to obtain temperature-time slope information, dT/dt . Base heating rates were computed from

$$Q_{\text{BASE}} = \frac{C_p M}{A} \frac{dT}{dt} + \frac{\epsilon \sigma T^4}{3600}, \text{ Btu/ft}^2\text{-sec}$$

where C_p = specific heat, $0.094 \text{ Btu/lb-}^\circ\text{F}$; M = mass of slug, lb ($0.625 \text{ in. diam} \times 0.1 \text{ in. depth}$); $\rho = \rho A t$, ρ = density, 558 lb/ft^3 ; ϵ = surface emissivity, 0.8 ; and σ = Stefan-Boltzman constant, $0.1713 \times 10^{-8} \text{ Btu/ft}^2\text{-hr-}^\circ\text{R}^4$

Final reduced data are presented in Figs. 1 and 2 for the steep and shallow trajectory flights, respectively. The expected heating rate curves shown in these figures are empirical, and were derived from the results of Ref. 1, which presents the heating ratio, $Q_{\text{BASE}}/Q_{\text{CONE}}$, for cold wall heating, as a function of base radial position for limiting values of sharp and blunt-cone vehicles. Previous theoretical and design experience suggests that effects of such parameters as vehicle geometry, heatshield, and type of flow can be empirically correlated very effectively with local cone heating rates prior to separation for

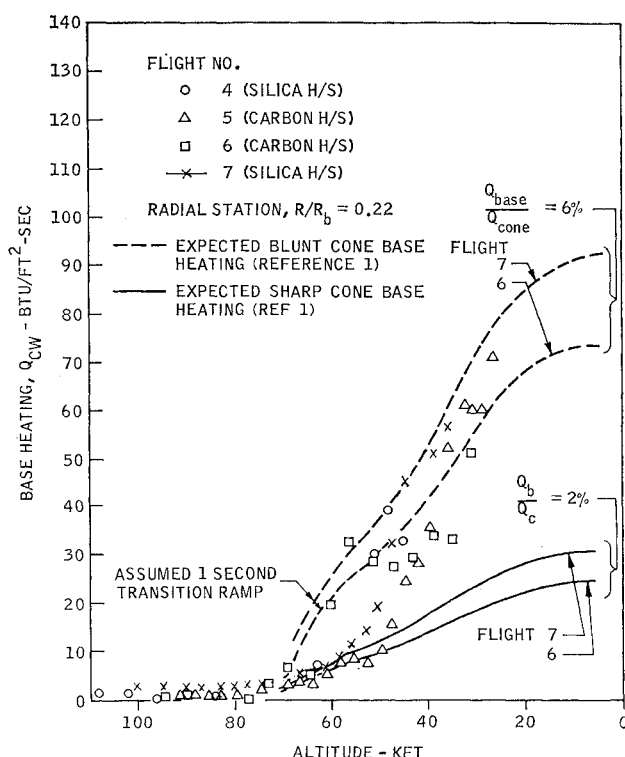


Fig. 1 Vehicle base heating-steep trajectories.

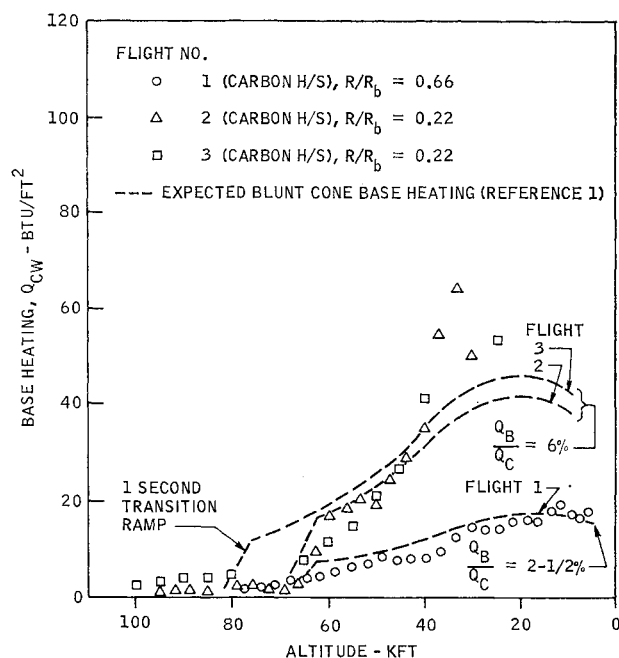


Fig. 2 Vehicle base heating-shallow trajectories.

Table 1. Nominal initial re-entry trajectory conditions

Trajectory	Altitude kft	Velocity fps	Path Angle deg
Shallow (3)	250	15,400	22
Steep (4)	250	16,700	40

Received January 17, 1972; revision received March 15, 1972.
Index category: Fluid Dynamics.

* Principal Engineer, Re-entry Systems Operation.

the same wall temperature by such a procedure. The cone side wall heating rates (cold wall) used for the comparisons include blowing as well as bluntness effects.² The effect of degree of bluntness is not included. Therefore, comparisons are made here only to indicate that the anticipated sharpness of the present vehicles is not valid.

The effective bluntness of these slender vehicles is quite noticeable even at the aft end of the vehicle. This is verified by the base heating data of Fig. 1 in which the expected heating for blunt and sharp vehicles is compared. The predicted heating of flights 6 and 7 covers the range of dispersion due to trajectory and heatshield material variations expected for all

four steep trajectory flights for which data are presented. The actual data are in general agreement with the base heating results on a 30% blunt vehicle rather than the expected theoretically sharp vehicle. Subsequent boundary layer calculations, however, indicate that the effects of the nose shock wave are felt to the end of these slender vehicles, as in the case of a blunt vehicle.

References

- ¹ Francis, W. L. and Davey, W. T., "Base Heating Experiments on Slender Cones in Hypersonic Flow," IAS Paper 62-179, IAS National Summer Meeting, Los Angeles, Calif, June 19-22, 1962.
- ² Sherman, M. M., "HT25F Cone Boundary Layer Program," METN 115, Aug. 1967, Aeronutronic Div., Philco-Ford Corp. Newport Beach, Calif.

Correlations of Peak Heating in Shock Interference Regions at Hypersonic Speeds

J. WAYNE KEYES* AND DANA J. MORRIS*

NASA Langley Research Center, Hampton, Va.

Nomenclature

BS, IP, IS, SL, TS	= bow shock, impingement point, impinging shock, shear layer, and transmitted shock, respectively, Fig. 1
C	= constant in Eq. (1)
c_p	= specific heat at constant pressure
h	= heat-transfer coefficient
M	= Mach number
n	= exponent in Eqs. (1, 2, or 3)
N_{Pr}	= Prandtl number
p	= pressure
R	= Reynolds number
T	= temperature
u	= velocity
X_{SL}	= shear layer length
γ	= ratio of specific heats
ρ	= density, note: ($\rho_w \propto p_p/T_w$)
μ	= viscosity
δ_{SL}	= shear-layer thickness
θ_{SL}	= shear-layer angle relative to local surface inclination

Subscripts

1, 2, 3, 4, 5	= regions in flow pattern Fig. 1
p	= peak value
w, ∞	= wall and freestream, respectively
u, s	= undisturbed and stagnation, respectively

Introduction

KNOWLEDGE of the peak heating in interference flow regions is necessary for the design of hypersonic configurations such as the space shuttle. Typical areas of interference flows on the shuttle include the flow between the mated booster and orbiter, and the fuselage bow shock impingement on the leading edges of wings and fins. An ex-

Received March 13, 1972; revision received May 4, 1972.

Index categories: Boundary Layers and Convective Heat Transfer-Turbulent; Supersonic and Hypersonic Flow; Jets, Wakes, and Viscid-Inviscid Flow Interactions.

* Aerospace Technologists, Viscous Flows Section, Hypersonic Vehicles Division.

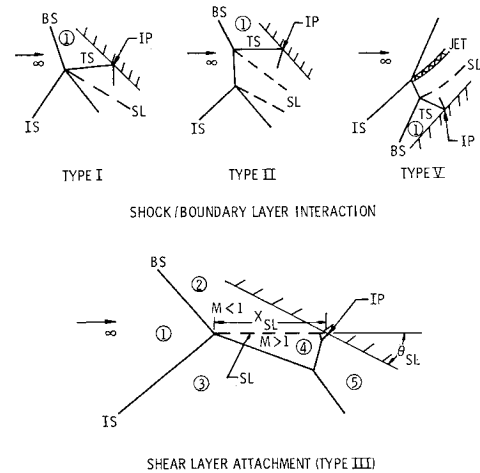


Fig. 1 Shock interference patterns.

tensive survey of the state of the art concerning various types of interference flows was made by Korkegi.¹ Edney² showed that increases in heating in shock interference regions result from one or more of the following mechanisms: shock/boundary-layer interaction, free shear layer attachment, and supersonic jet impingement. Correlations of peak heating due to shock/boundary-layer interactions for laminar, transitional, and turbulent flows were obtained by Markarian.³ Back and Cuffel⁴ correlated changes in turbulent heat transfer due to shock wave impingement and flow expansion around a corner. Peak heating for turbulent separated flow on wedges was correlated by Holden.⁵ Nestler⁶ and Bushnell and Weinstein⁷ used the concept of shear layer attachment in correlating peak heating for separated flows in the reattachment region.

This Note presents correlations of measured pressure and heat-transfer peaks for shock/boundary-layer interactions and shear layer attachment on configurations with both two-dimensional and three-dimensional interactions. The peak values were obtained in an extensive investigation of shock interference heating⁸ on hemispheres, a 30° included angle wedge, and a 2.54 cm diam cylindrical leading edge fin model. The investigation included data for Mach numbers of 6 and 20 over a freestream Reynolds number range from 3.3-25.6 million per meter and specific heat ratios of 1.4 and 1.67. Flat plate shock generator angles varied from 5° to 25°. Sketches of the types of shock interference patterns as classified by Edney and discussed in the present analysis are shown in Fig. 1.

Shock/Boundary-Layer Interaction

The maximum increase in heating is at the impingement point IP of the transmitted shock (TS shown in Fig. 1). Murphy⁹ conducted a critical evaluation of methods used to predict both the pressure and heat-transfer distributions through the interaction region. The most useful approach from a practical standpoint is that of Markarian,³ who proposed empirical correlations based upon the inviscid pressure rise across the interaction region. These correlations are well-suited for rapid engineering calculations, assuming the peak pressure is known. The expression is of the form

$$h_p/h_u = C[p_p/p_u]^n \quad (1)$$

where C and n depend upon whether the interaction is laminar, transitional, or turbulent. Figure 2a shows the correlation of peak pressures and heat transfer obtained in the present investigation for the wedge and fin models. These peaks are in good agreement with the Markarian correlation curve for a laminar interaction ($C = 1$ and $n = 1.29$). In the present case, the boundary layers in the impingement region are believed to be laminar. Extensive boundary-layer separation